Molecular Pharmacology Fast Forward. Published on February 15, 2011 as doi:10.1124/mol.110.069831
This article has not been copyedited and formatted. The final version may differ from this version.

MOL #69831

Early failure of *N*-Methyl-D-aspartate receptors and deficient spine formation induced by reduction of regulatory heme in neurons.

Tatyana Chernova, Joern R. Steinert, Paul Richards, Rajendra Mistry, R.A. John Challiss, Rebekah Jukes-Jones, Kelvin Cain, Andrew G. Smith, and Ian D. Forsythe

MRC Toxicology Unit, University of Leicester, Leicester, United Kingdom (T.C., J.R.S P.R., A.G.S., R.J-J, K.C., I.D.F); and Department of Cell Physiology and Pharmacology (R.M., R.A.J.C.), University of Leicester, Leicester, United Kingdom

Molecular Pharmacology Fast Forward. Published on February 15, 2011 as DOI: 10.1124/mol.110.069831
This article has not been copyedited and formatted. The final version may differ from this version.

Running title: Deficiency of regulatory heme causes NMDA receptor failure

Correspondence should be addressed to

Tatyana Chernova
MRC Toxicology Unit
Hodgkin Building
University of Leicester
Lancaster Road
Leicester
LE1 9HN
Tel. 0116 252 5618
Fax 0116 252 5616
tc28@le.ac.uk

The number of text pages 31,

Number of figures – 8 and 2 supplemental,

Number of references- 40,

Abstract- 250 words,

Introduction- 535 words,

Discussion –1470 words.

Abbreviations:

(NMDAR) - *N*-Methyl-D-aspartate receptor

(ERK1/2) - extracellular signal-regulated kinase 1/2

(ALAD) - aminolevulinic acid dehydratase

(ALAS) - aminolevulinic acid synthase

(nNOS)Neuronal nitric oxide synthase

Molecular Pharmacology Fast Forward. Published on February 15, 2011 as DOI: 10.1124/mol.110.069831
This article has not been copyedited and formatted. The final version may differ from this version.

Abstract

An initial stage of many neurodegenerative processes is associated with compromised synaptic function and precedes synapse loss, neurite fragmentation and neuronal death. Previously we showed that deficiency of heme, regulating many proteins of pharmacological importance, causes neurodegeneration of primary cortical neurons via *N*-Methyl-D-aspartate receptor (NMDAR)-dependent suppression of the extracellular signal-regulated kinase 1/2 (ERK1/2) pathway. Here we asked if reduction of heme causes synaptic perturbation prior to neurite fragmentation in neuronal cultures and investigated molecular mechanisms of synaptic dysfunction in these cells. We showed the change in the NR2B subunit phosphorylation that correlates with compromised NMDAR function after reduction of regulatory heme and a rapid rescue of NR2B phosphorylation and NMDAR function by exogenous heme. Electrophysiological recordings demonstrated diminished NMDAR currents and NMDAR-mediated calcium influx after 24 hours of inhibition of heme synthesis. These effects were reversed by treatment with heme; however, inhibition of the Src family kinases abolished the rescue effect of heme on NMDA-evoked currents. Diminished NMDAR current and Ca^{2+} influx resulted in suppressed cGMP production and impairment of spine formation. Exogenous heme exerted rescue effects on NR2B tyrosine phosphorylation and NMDA-evoked currents within minutes, suggesting direct interactions within the NMDAR complex. These synaptic changes following inhibition of heme synthesis occurred at this stage without apparent dysfunction of major hemoproteins. We conclude that regulatory heme is necessary in maintaining NR2B phosphorylation and NMDAR function. NMDAR failure occurs prior to neurite fragmentation and may be a causal factor in neurodegeneration; this could suggest a route for an early pharmacological intervention.

Molecular Pharmacology Fast Forward. Published on February 15, 2011 as DOI: 10.1124/mol.110.069831
This article has not been copyedited and formatted. The final version may differ from this version.

Introduction

Neurodegeneration progresses from reversible down-regulation of synaptic function to irreversible synapse loss and neuronal death, so rescue at such an early stage of synaptic loss offers an attractive approach for therapeutic intervention (Mallucci, 2009; Wishart et al., 2006). Elucidating mechanisms causing neurodegenerative process requires capturing an earlier synaptic perturbation, which is not always easy in existing *in vivo* and *in vitro* models of neurodegeneration (Boekhoorn et al., 2006; Soto and Estrada, 2008). Here we focus on early stages of synaptic dysfunction prior to neurite fragmentation in primary neurons with reduced level of heme and on identifying factors triggering synaptic loss that has greater potential to facilitate pharmacological strategies to reverse neurodegeneration.

Deficiency of heme is detrimental to neurons and is a contributory factor in cell ageing (Chernova et al., 2006), Alzheimer's disease (Atamna and Frey, 2004) and drug-induced neurotoxicity (Meyer et al., 2005). It also diminishes neuron-specific gene expression, alters cellular signalling and induces apoptosis (Zhu Y, 2002). Heme synthesis is up-regulated during differentiation of cultured neuronal cells (Shinjyo and Kita, 2006) and exogenous heme promotes outgrowth of neurites (Ishii and Maniatis, 1978). Heme exists in at least two pools in cells: heme bound within hemoproteins and "free" heme, *i.e.* not associated with a protein. A portion of the unbound heme forms a regulatory pool that mediates a signalling role through binding to heme-regulatory motifs in proteins and modulating their functions; this includes ion channels (Tang et al., 2003), transcription factors (Ogawa et al., 2001) and nuclear receptors (Raghuram et al., 2007). Previously, we demonstrated that heme is necessary to maintain neurite integrity, while heme deficiency causes neurodegeneration via NMDA receptor (NMDAR)-dependent suppression of the ERK1/2 pathway. Heme deficient cultured neurons displayed progressive neurite fragmentation followed, eventually, by cell death. The rescue of pro-survival ERK1/2 activation by heme was mediated predominantly via the NR2B-containing NMDARs (Chernova et al., 2007). These observations were made in neurons chronically deficient in heme where loss of both bound and regulatory heme pools might have contributed to the progressive fragmentation of neurites.

Molecular Pharmacology Fast Forward. Published on February 15, 2011 as DOI: 10.1124/mol.110.069831
This article has not been copyedited and formatted. The final version may differ from this version.

Here we tested the hypothesis that heme is necessary for the regulation of NMDAR and that a lack of "free" heme rapidly causes this ion channel dysfunction. We have examined the early stage of heme deficiency in cortical cultures and identified an early NMDAR impairment. Failure of NMDAR function occurred shortly (16-24 h) after reduction of regulatory heme and was reflected by markedly decreased NMDAR currents and Ca^{2+} influx. This correlated with a reduction in the phosphorylation of the NR2B subunit of NMDARs. Additionally, NMDAR-dependent cGMP production was compromised and dendritic spine formation reduced. Exogenous heme rescued the ion channel function and spine formation, but only if normal levels of NR2B phosphorylation were resumed. We have demonstrated that heme modulates NMDAR function and tyrosine phosphorylation of NR2B subunit within minutes in a signalling mode and requires SFKs activity. Heme bound to major hemoproteins was preserved and the functions of tested proteins were unaffected. These findings suggest that early synaptic impairment following inhibition of heme synthesis is caused by reduction of regulatory heme. We conclude that NMDAR failure occurs prior to neurite fragmentation at the early stage of heme deficiency and may be a causal factor in neurodegeneration.

Molecular Pharmacology Fast Forward. Published on February 15, 2011 as DOI: 10.1124/mol.110.069831
This article has not been copyedited and formatted. The final version may differ from this version.

Materials and Methods

Primary cell culture. Primary cortical neurons were prepared from either male or female 14-day-old fetuses of the BALB/c mouse strain bred in-house. The isolated neocortex of embryos was gently dissociated to release the neurons, which were washed twice in Neurobasal medium (GIBCO, Carlsbad, CA) supplemented with 10% foetal calf serum. Cell suspensions were plated on poly-L-lysine-coated 35-mm plates at a density of 1 x 10^6 cells per dish. After attachment of the cells, the plating medium was changed to serum-free culture medium containing 96% (v/v) Neurobasal medium (GIBCO), 2 µM GlutaMAX, 2% B-27 supplement (GIBCO/Invitrogen, Paisley, UK), 100 µg/mL streptomycin, and 100 U/mL penicillin. Viability of the cells was estimated by the trypan blue exclusion assay and typically was around 85%. After 5 days, 10µM cytosine arabinoside (*1β*-arabinofuranosylcytosine) was added to the culture medium for 3 days to stop proliferation of glial cells or fibroblasts. The cells were grown in a humidified incubator at 37° C (95% room air/5% CO_2). Selective inhibitor of SFKs PP2 [4-amino-5-(4-chlorophenyl)-7-(*t*-butyl)pyrazolo[3,4-*d*]pyrimidine] (Calbiochem) was applied at 50nM for 24 h to control cells and to the treated cell treated with SA +/- heme, or for 2 h in 2-h heme readmission subsequent to SA treatment.

Inhibition and readmission of heme, measurement of cellular heme content and heme synthesis. To inhibit heme synthesis, cells were cultured in serum-free medium with 250µM succinyl acetone (SA) (4,6-dioxoheptanoic acid) (Sigma, Dorset, UK) for the stated durations. For heme readmission experiments, cells were treated daily with 100 nM hemin (iron protoporphyrin IX); stock solution was added to human serum albumin in a 1:1 molar ratio before treatment. The heme concentrations were verified spectrophotometrically.

Total cellular heme was measured by using a modified QuantiChrom Heme Assay (BioAssay Systems, Hayward, CA, USA). The OD measurements were taken using The NanoDrop 2000 Spectrophotometer (Thermo Fisher Scientific, Wilmington, DE, USA). The amount of heme in each sample was expressed as µmol heme per mg of total protein. For measurement of heme synthesis, cells were incubated with

Molecular Pharmacology Fast Forward. Published on February 15, 2011 as DOI: 10.1124/mol.110.069831
This article has not been copyedited and formatted. The final version may differ from this version.

0.4 μCi of [3,5- ^{3}H]aminolevulinic acid hydrochloride (ALA; 2.6 Ci/mmol; PerkinElmer, Boston, MA) for 24 h. Heme was extracted from the cells by acetone-HCl and diethyl ether. The amount of radioactivity in extracted heme was measured by scintillation counting as described previously (Chernova et al., 2007) . Total recovery of radioactivity from all fractions was the same for treated and untreated cells.

RNA extraction and quantitative real-time PCR analysis. Total RNA was isolated from treated and untreated cells at different time points by using TRI-reagent (Sigma, Dorset, UK) and cDNA synthesis was performed using random primers and Superscript II (Invitrogen). PCR primers were selected using the Primer Express version 2.0 Software program (Applied Biosystems, Foster City, CA). Primers sequences were as follows: β-actin forward primer, 5'-GATTACTGCTCTGGCTCCTAGCA-3', reverse primer, 5'-GTGGACAGTGAGGCCAGGAT-3'; δ-aminolevulinate synthase 1 (*ALAS1*) forward primer, 5'-TCTTC-CGCAAGGCCAGTCT-3', reverse primer, 5'-TGGGCTTGAGCAGCCTCTT-3'; *CYP4x1* forward primer 5'–CCTGGACATAATAATGAAATGTGCTT-3'; reverse primer, 5'-CTTCACGTAAGACTCATAGGTGCC-3';

Primers were designed to cross exon–exon boundaries. PCR was performed using SYBR Green PCR Master Mix, primers, and 10 ng of reverse-transcribed cDNA in the ABI PRISM 7700 Sequence Detection System (Applied Biosystems, Foster City, CA) as described previously (Kannan et al., 2010) . Quantification was performed using the comparative CT method (ΔΔCT). Data are presented as the mean ± SD (n = 3–8 for each group). Statistical significance was assessed as $p < 0.05$ using one-way ANOVA.

Immunocytochemistry. After treatment, cells were fixed with 4% paraformaldehyde at room temperature for 20 min and permeabilized with 0.2% Triton X-100 (Sigma, Dorset, UK) in PBS for 5 min. Cells were then incubated with rabbit anti-phospo-NR2B (Tyr 1252 or Tyr 1336) (R&D Systems, Abingdon, UK) and mouse anti-PSD-95 antibody (NeuroMab, Davis, CA, USA) at room temperature for 1 h. Secondary antibodies (goat anti-rabbit Alexa Fluor 546 and goat anti-mouse Alexa Fluor 488 at

Molecular Pharmacology Fast Forward. Published on February 15, 2011 as DOI: 10.1124/mol.110.069831
This article has not been copyedited and formatted. The final version may differ from this version.

1:500) were then added for 1h, followed by nuclear staining with 300 nM 4'-6-diamidino-2-phenylindole (DAPI) for 10 min. Secondary antibodies alone were used as specificity controls and uniformly resulted in very low background levels of fluorescence.

Transfection of cortical neurons. At 7DIV, neurons were transfected with plasmids expressing FLAG-tagged tdTomato as a cell fill provided by Dr. Michael J. Schell (Dept. of Pharmacology, Uniformed Services University, Bethesda) to visualize dendritic morphology. A total of 0.5μg DNA and 1μLLipofectamine2000 (Invitrogen) was premixed according to the manufacturer's instructions, and added to cultures (0.5x 10^6 cells) growing on bottom glass chambers (Fisher Scientific, Loughborough, UK) in 900μL of medium. After 6 h the medium was replaced with a fresh 900μL of serum-free Neurobasal medium supplemented as described above. Transfection efficiency was estimated to be less than 2%. Neurons were imaged at 13DIV.

Imaging and quantification of spines. Cortical neurons with pyramidal morphology were selected for analysis from the transfected cell population. Images of cultured cells were obtained with a Zeiss LSM 510 META confocal microscope equipped with a 63x oil immersion lens. Images were collected as a series of Z sections (approx. 0.5 micron). Images were reconstructed using Volocity software (Improvision, Coventry, UK). Total protrusions from the dendrite (spines) were quantified over unit length and expressed as number per 10 μm of the neurites. Only fields with a low density of transfected neurons were used to quantify the spines length and number.

Immunoblotting. Proteins were extracted from primary neurons using NP-40 lysis buffer (1%NP-40, 20mM Tris-HCl pH8.0, 137mMNaCl, 10%glycerol, 2mM EDTA, 1mM sodium orthovanadate, 10 μg/μL leupeptin, 10 μg/μL aprotinin) and brief sonication. Microsomal fraction was prepared as described previously (Kapoor et al., 2006). Briefly, the cells where scrapped in PBS and then pelleted by centrifuging at 200×g for 10 min. The cell pellet was resuspended in microsomal dilution buffer containing 0.1(v/v) glycerol, 0.25 mM PMSF, 0.01MEDTA and 0.1 mM DTT. Following brief sonication, the cells were centrifuged at 9000×g for 20 min. The supernatant was then further

Molecular Pharmacology Fast Forward. Published on February 15, 2011 as DOI: 10.1124/mol.110.069831
This article has not been copyedited and formatted. The final version may differ from this version.

centrifuged at 105,000×g for 60 min, to isolate the microsomes. The microsomal pellet was resuspended in microsomal dilution buffer and used for analysis. Separation by SDS-PAGE or native PAGE (for nNOS detection) was followed by immunoblotting and enhanced chemiluminescence detection (GE Healthcare, Little Chalfont, UK). Antibodies were from the following sources: NMDAR NR1, total NR2B from Santa Cruz Biotechnology (Santa Cruz, CA); NMDAR phospho-NR2B Y1252 and Y1336 from (R&D Systems, Abingdon, UK), α-tubulin from Sigma (Dorset, UK), ALAS1 from Abcam (Cambridge, UK), HO-1 and P450 reductase antibodies were from Stressgen (Victoria, Canada), CYP1A1 was from Cambridge Bioscience (Cambridge, UK) and CYP4X1 was from Dr D. Bell (School of Biology University of Nottingham). Blots were subsequently exposed to a second primary antibody against α-tubulin, to verify equivalent protein loading and transfer. Bands were detected by enhanced chemiluminescence (GE Healthcare, Buckinghamshire, UK), exposed to X-ray films under nonsaturating conditions. Results were quantified using densitometry and Image Quant 5.2 software. All comparisons were made within blots. Statistical significance was estimated using two-tailed Student's *t* test.

NMDA application. Agonist application experiments on primary cortical cultures were performed using a Picospritzer III (Intracel, Frederick, MD) connected to a patch electrode filled with artificial cerebrospinal fluid (aCSF) containing 100 μM NMDA (Sigma, Dorset, UK). The tip of the electrode was placed near a patch-clamped cortical neuron, and the maximal response to the agonist was optimized by adjusting the pipette position. Puffs were applied for 30 ms every 8 s (20 psi) in the presence of (6,7-dinitroquinoxaline-2,3-dione) (DNQX, 10 μM), D-serine (10 μM), and bicuculline (10 μM). No extracellular Mg^{2+} was added to these solutions. To create a current–voltage (*I–V*) relationship for NMDA-evoked currents, we applied NMDA while holding at different potentials ranging from –60 to +40 mV.

Electrophysiology. Whole-cell patch-clamp recordings were made from primary cultures of cortical neurons [visualized at 60x with a Nikon E600FN (Tokyo, Japan) fitted with differential interference

Molecular Pharmacology Fast Forward. Published on February 15, 2011 as DOI: 10.1124/mol.110.069831
This article has not been copyedited and formatted. The final version may differ from this version.

contrast optics] using a multiclamp 700B amplifier (Molecular Devices) and pClamp9 software (Molecular Devices). Data were sampled at 50 kHz and filtered at 10 kHz. Patch pipettes were pulled from borosilicate glass capillaries (GC150F-7.5; Harvard Apparatus, Edenbridge, UK) using a two-stage vertical puller (PC-10; Narishige, Tokyo, Japan). Tips were polished (Micro Forge; Narishige), and pipettes had a final open-tip resistance of ~5 MΩ when filled with a patch solution containing the following (in mM): 130 CsCl, 10 HEPES, 5 EGTA, and 1 $MgCl_2$, pH adjusted to 7.2 with CsOH. Whole-cell access resistances were <20 MΩ. Bath solution was without extracellular [Mg^{2+}] and as follows (in mM): 135 NaCl, 3 KCl, 10 HEPES, 2 $CaCl_2$, 10 glucose, and 45 sucrose. Where specified, heme was added to the bath solution or directly to the pipette solution at 0.1 μM.

Ca^{2+} imaging. For $[Ca^{2+}]_i$ determinations, sub-confluent cortical neurons were cultured on glass coverslips and loaded for 10 min at room temperature with 5 μM fura 2-AM (Invitrogen) aCSF. After loading, cells were kept in aCSF for up to 1 h. Fluorescence was measured using a computer-controlled Polychrome II Monochromator (T.I.L.L. Photonics, Martinsried, Germany) with excitation at 340, 360 and 380 nm and emission detected at >505 nm. The ratio of fluorescence at 340 and 380 nm excitation was used as a measure of $[Ca^{2+}]_i$. Fluorescence was detected using a CCD pentamax camera (Princeton Instruments, Trenton, NJ). Data were recorded and analyzed using Meta Imaging (series 7.0) software (Molecular Devices, Sunnyvale, CA). A pair of images was obtained every second with 20 ms exposure time at each wavelength. Fluorescence measurements were preformed in the cell soma. Only cells with low resting ratios (<0.6) and cells that returned to basal ratios after stimulation were used for analysis.

Radio-immunoassay of cyclic GMP. Control, NO-donor S-nitroso-N-acetylpenicillamine (Sigma, Dorset, UK) stimulated or NMDA stimulated (10 min, 100 μM and 50μM, respectively) cortical cultures were used for assessing cGMP production. Briefly, the SOC was isolated and neutralized tissue extracts were diluted five-fold in 100mM sodium acetate, pH 6.2 and acetylated by consecutive addition of triethylamine (10μL) and acetic anhydride (5μL) and used in the radioimmunoassay (Brooker et al., 1979) within 60 min. Cyclic GMP standards (100μL; 0-4nM) were treated identically. Acetylated

Molecular Pharmacology Fast Forward. Published on February 15, 2011 as DOI: 10.1124/mol.110.069831
This article has not been copyedited and formatted. The final version may differ from this version.

samples (100μL) were mixed with 2'-*O*-succinyl 3-[^{125}I]-iodotyrosine methyl ester cyclic GMP (GE Healthcare, IM107) (50μL, ~3,000 d.p.m. made up in 50mM sodium acetate, 0.2% bovine serum albumin (BSA), pH 6.2) and 100μL of anti-cyclic GMP antibody (GE Healthcare, TRK500; diluted in 50mM sodium acetate, 0.2% BSA, pH 6.2). Samples were intermittently vortex-mixed during a 4 h incubation at 4^{o}C. Free and bound cyclic GMP was separated by charcoal precipitation with 500μL of a charcoal suspension (1% (w/v) activated charcoal in 100mM potassium phosphate, 0.2% BSA, pH 6.2). After vortex-mixing for 5 min samples were centrifuged (13,000 g, 4 min, 4^{o}C) and radioactivity determined in an aliquot of supernatant (600μL). Unknown values were determined from the cyclic GMP standard curve using GraphPad Prism 4 (GraphPad Software Inc., San Diego, CA).

Detection of mitochondrial membrane potential (ΔΨm).Mitochondrial membrane potential was detected using DePsipher™ Kit for Detection of Mitochondrial Membrane Potential Disruption (R&D Systems Inc., USA) according to manufacturer's instructions. Lipophilic Cationic dye 5,5',6,6'-tetrachloro-1,1',3,3'-tetraethylbenzimidazoyl carbocyanine iodide enters the inner mitochondrial matrix in its monomeric form when the mitochondrial membrane is polarized. When the mitochondrion has a high ΔΨm, the dye crosses the membrane and forms aggregates, which appear red under UV light. Living neurons were stained and observe immediately with a microscope using a long-pass filter (fluorescein and rhodamine). In healthy cells, the mitochondria were stained red following aggregation of the DePsipher within the mitochondria. In cells with disrupted ΔΨm, the dye remains in its monomeric form in the cytoplasm and appears entirely green.

Measurement of ATP in neurons. Cultured neurons were treated with 250μM SA for 1-6 days and harvested at 12DIV. The level of cellular ATP in neurons was determined with a luciferase-based CellTiter-Glo Luminescent Cell Viability Assay (Promega Corp., Madison, WI), according to the manufacturer's recommendations. After the plates were developed, luminescence was measured in a microplate luminometer (Luminoskan; Labsystems, Helsinki, Finland). Each set of data was collected from multiple replicate wells of each experimental group from 5 independent experiments; the

Molecular Pharmacology Fast Forward. Published on February 15, 2011 as DOI: 10.1124/mol.110.069831
This article has not been copyedited and formatted. The final version may differ from this version.

concentrations were normalized against total cellular protein and expressed as nmol per mg of protein (mean± SD).

Results

Inhibition of heme synthesis promptly reduced regulatory pool of intracellular heme.

To examine the chronology of the neuronal deficit with reduced heme we inhibited its synthesis for 1-6 days by treatment with 250μM succinylacetone (SA), a specific inhibitor of aminolevulinic acid dehydratase (ALAD) (Sassa and Nagai, 1996) . Heme synthesis was reduced by about 50% (Figure 1A), causing 17% ±6% decrease of total intracellular heme (Figure 1B). This reduction was accompanied by a marked increase in the expression of *ALAS1* (Figure 1C), the gene encoding aminolevulinic acid synthase, which is under negative transcriptional feedback control by the regulatory pool of intracellular heme (Sassa, 2004; Sassa and Nagai, 1996). The up-regulation of *ALAS1* expression in SA-treated neurons indicated that the decrease in heme was physiologically significant, and this was a rapid process, occurring within hours after inhibition of synthesis. After 16 h of SA treatment *ALAS1* mRNA increased two-fold, similar to the up-regulation observed in chronically-deficient neurons (Chernova et al., 2006). An increased amount of ALAS1 protein in response to reduced heme levels was detected in these SA-treated cultures (Figure 1D), consistent with previously shown regulation by “free” heme via alterations in protein half-lives (Zheng et al., 2008). By contrast, when heme was added back to SA-treated cells there was a 24 ± 2% increase in intracellular heme, accompanied by a decrease in *ALAS1* expression, again consistent with a regulated physiological response (Figure 1 B, C). Our results suggest that the regulatory pool of heme was compromised within hours if *de novo* synthesis was inadequate. We examined how a lack of regulatory heme affected neuronal function, and tested if NMDAR was compromised in neurons with reduced regulatory heme. We chose a 24h time-point of heme synthesis inhibition as this corresponded to the depleted regulatory heme pool, reflected by a two-fold up-regulation of *ALAS1*, and a relatively small (17%) reduction of total cellular heme.

Molecular Pharmacology Fast Forward. Published on February 15, 2011 as DOI: 10.1124/mol.110.069831
This article has not been copyedited and formatted. The final version may differ from this version.

Reduction of intracellular heme decreases tyrosine phosphorylation of NR2B

Although chronically heme-deficient neurons have reduced expression of NMDAR subunits at the stage of neurite loss (Chernova et al., 2007), the initial changes following inhibition of heme synthesis do not involve down-regulation in gene or protein expression for NMDAR subunits NR1 and NR2B (Supplemental figure 1 A-D). NR2B is a major tyrosine-phosphorylated protein regulated by Src family kinases (SFKs) in the postsynaptic density (Moon et al., 1994) and is impaired in heme-deficient neurons (Chernova et al., 2007). To examine the early changes caused by reduced heme availability we used immunoblotting and immunostaining to monitor NR2B phosphorylation at Tyr1336 and Tyr1252 in the presence or absence of SFKs inhibitor PP2 and heme, in neurons treated with SA for 24 h, the time-point when the two-fold up-regulation of *ALAS1* indicated a depletion of the regulatory heme pool (Figure 2 A-N). Phosphorylation of NR2B at Tyr1336 and Tyr1252 was diminished in neurons by incubation with PP2 and was markedly lower in SA-treated compared to control cultures (Figure 2A, 2B). PP2 and SA treatments had additive effects on the reduction in Tyr1336 and Tyr1252 phosphorylation (Figure 2A, 2B). In cultures co-treated with SA and heme, phosphorylation of Tyr1336 and Tyr1252 was unaffected (Figure 2A, 2B). The rescue effect by exogenous heme was abolished if these cultures were concomitantly treated with PP2 (Figure 2A, 2B). The levels of NR2B protein phosphorylated at Tyr1336 and Tyr1252 were also examined by immunostainig of neuronal cultures under the same conditions (Figure 2 C-N). Together these data provide strong evidence that compromised availability of heme impairs NR2B subunit phosphorylation and this is an early event in heme deficiency-induced neurodegeneration. This raises the question as to whether the functional outputs of NMDARs are also affected at this early stage?

NMDAR current is promptly impaired by reduction of intracellular heme.

Molecular Pharmacology Fast Forward. Published on February 15, 2011 as DOI: 10.1124/mol.110.069831
This article has not been copyedited and formatted. The final version may differ from this version.

Phosphorylation of NMDAR regulates the channel kinetics and the Ca^{2+} permeability as well as membrane localization and trafficking (Cull-Candy and Leszkiewicz, 2004). Following the finding of altered NR2B subunit phosphorylation after reduction of cellular heme, we examined how the NMDAR current was affected by changes of heme concentration. Whole-cell patch-clamp recordings were made from single cortical neurons maintained in dissociated culture (12DIV) and treated with SA for 24 h in the presence or absence of heme. Reduction of intracellular heme for 24 h decreased NMDA-mediated whole-cell currents compared to control cultures (Figure 3A, top [Ctrl] *versus* upper middle traces [24h SA]). Neurons co-treated with SA and heme for the same time exhibited larger responses to NMDA application (Figure 3A, lower middle traces [24h SA+H]). Incubation of control cultures with 100nM heme for 24 h did not have an effect on NMDA-evoked whole-cell current (Figure 3A, bottom traces [24h H]). Data summarized in Figure 3B show I/V curves for neurons under control conditions, heme treatment, SA treatment and SA treatment in the presence of heme. NMDA-evoked currents at 40mV holding potential were suppressed after SA treatment and this effect was reversed by co-treatment with heme (Figure 3C). The rescue effect of heme on NMDAR current was abolished in heme deficient cultures co-treated with SFKs inhibitor PP2 (Supplemental Figure 2 A-C). The results suggest that the impairment of NMDAR function in neurons with reduced heme is associated with compromised phosphorylation of the regulatory NR2B subunit.

Ca^{2+} influx through NMDARs is reduced in neurons with low intracellular heme levels.

Since NMDARs are highly Ca^{2+} permeable (Viviani et al., 2006), we monitored changes in intracellular Ca^{2+} in response to NMDA application, as a further index of channel function. Cultures (12DIV) were loaded with Fura 2-AM and imaged using a CCD camera; NMDA was pressure applied onto control or SA-treated (24-44h) cultures. The ratio of fluorescence at 340 and 380 nm excitation was used as a measure of intracellular Ca^{2+} ($[Ca^{2+}]_i$). Basal $[Ca^{2+}]_i$ did not change in SA treated cultures (data not shown), whereas response to NMDA application

Molecular Pharmacology Fast Forward. Published on February 15, 2011 as DOI: 10.1124/mol.110.069831
This article has not been copyedited and formatted. The final version may differ from this version.

was affected. SA-treated neurons showed diminished Ca^{2+} influx (Figure 4A) in response to NMDA (Δ ratio calculated as peak ratio minus basal ratio). Peak Ca^{2+} responses were reduced at all time-points of SA treatment (Figure 4B). Heme readmission during 24h of SA treatment recovered the peak Ca^{2+} responses to control levels (Figure 4B). The data confirm that NMDAR function is affected within 24 h after inhibition of heme biosynthesis.

NMDAR-dependent production of cGMP is affected by reduction of intracellular heme.

Neuronal nitric oxide synthase (nNOS) is activated by Ca^{2+}influx through NMDAR, leading to downstream production of cGMP following NO activation of soluble guanylate cyclase. Production of cGMP in response to NMDAR stimulation in cultures with low heme was significantly reduced by 22±2 % compared to control cultures (Figure 4C). The response to NMDA was affected after 16 h of inhibition of heme synthesis, and as NMDAR function declined with longer SA treatment, so did cGMP production (by 38 ± 4% at 42 h after SA addition). These results provide further evidence of NMDAR functional impairment as an early change in the neurons with compromised availability of heme.

Heme deficiency reduces dendritic spine number.

Formation of dendritic spines by cortical neurons is closely associated with synaptic assemblies and plasticity and increased intracellular Ca^{2+} via NMDAR induces the formation and remodelling of dendritic spines (Ethell and Pasquale, 2005). Given the impaired NMDAR function we have observed in the neurons with reduced heme, we used imaging techniques to examine changes in dendritic spine formation. To visualize dendritic morphology neurons were transfected with FLAG-tagged tdTomato (red fluorescent cell fill) on 7DIV and then examined at 13DIV after treatment with SA or SA and heme for 24 h with or without addition of the SFKs inhibitor PP2. Cortical neurons with pyramidal morphology were selected for analysis from the transfected cell population. The number of spines per

Molecular Pharmacology Fast Forward. Published on February 15, 2011 as DOI: 10.1124/mol.110.069831
This article has not been copyedited and formatted. The final version may differ from this version.

10μM length of dendrite was significantly lower in the neurons with reduced cellular heme, whereas co-treatment of these cultures with heme reversed this phenomenon (Figure 5 A-C, F). Inhibition of SFKs abolished the rescue effect of heme (Figure 5E, 5F) but did not cause further deterioration in spine formation in SA-treated cultures (Figure 5D, 5E). These findings suggest a mechanistic link between failure of NMDAR and spine formation at early stage of heme deficiency and provide evidence that the rescue by heme is NR2B phosphorylation-dependent.

Heme modulates NMDAR function and NR2B phosphorylation within minutes.

To examine if the potentiation of NMDA-mediated current by heme is a signalling event, we conducted whole-cell patch clamp recordings simultaneously with re-introducing heme to the heme-deficient neurons and recorded for 13 minutes after which currents reached plateau levels under all recording conditions (Figure 6A). The neurons treated with SA for 24h showed a 60% reduction in NMDA-evoked currents (Figure 6A, blue diamonds) over a recording time of 13 minutes which is consistent with a dialysis process and a current run down. Heme was introduced into the bath solution after two minutes of recording and caused a 40% rise of the NMDAR current (red square; after an initial 2-minute decline prior to heme addition). When heme was present in the patching pipette, there was no initial decline and the increase of the current started immediately (Figure 6A, green triangles). At the13 min time-point NMDA-evoked currents were ~140% of initial currents values if heme was added to the bath, and ~110% if heme was present in the pipette. In contrast, in SA-treated cells currents were only ~40% of initial values after 13 minutes of recording. Comparison of the three curves showed that by 10 minutes exposure to heme the NMDAR current is 2-3 fold larger than in the absence of heme.

These alterations of the ion channel function correlated with the changes in NR2B phosphorylation levels upon re-admission of heme to heme-deficient neurons (Figure 6B, C). At a 15 min time-point NR2B phosphorylation of NR2B at Tyr1252 and Tyr1336 were recovered to control levels. However, if these neurons were pre-treated for 2h with PP2 the rescue effect of heme was abolished, similar to the

Molecular Pharmacology Fast Forward. Published on February 15, 2011 as DOI: 10.1124/mol.110.069831
This article has not been copyedited and formatted. The final version may differ from this version.

changes observed in cultures co-treated with heme and SA for 24h. These data show that regulation of NMDAR by heme is exerted rapidly and suggest a phosphorylation-dependent signalling mechanism.

Heme is preserved in major hemoproteins in neurons despite depletion of regulatory pool.

Depletion of heme from the regulatory pool clearly occurred within hours of SA treatment. We investigated what effect this treatment had on various hemoprotein functions in neurons?

Many mitochondrial proteins are hemoproteins, including those engaged in the electron transport chain and ATP generation. Mitochondrial membrane potential ($\Delta\Psi m$) and ATP generation were monitored after inhibition of heme synthesis to determine whether mitochondrial hemoproteins functions were affected in neurons when total cellular heme was reduced by ~17%. Inhibition of heme synthesis for at least 72 h had no effect on $\Delta\Psi m$ (Figure 7A, B), consistent with a well sustained ATP generation in SA-treated neurons. Further measurement of ATP concentration (up to 6 days of heme synthesis inhibition) revealed that mitochondrial function was also unaffected in these cultures (Figure 7C). These data show that heme was not depleted from mitochondrial hemoproteins under these conditions.

Soluble guanylate cyclase (sGC) is a hemoprotein, which on binding NO to heme increases cGMP production up to 300-fold (Ballou et al., 2002). sGC activation by the NO donor S-nitroso-N-acetylpenicillamine (SNAP) was measured as the ratio of basal to stimulated cGMP accumulation and was similar in control cultures and those treated with SA for 42 h (Figure 8A) demonstrating that the capacity of sGC to generate cGMP was unaffected.

The hemoprotein neuronal nitric oxide synthase (nNOS) catalyzes the NADPH-dependent oxidation of L-arginine to citrulline and NO (White and Marletta, 1992). nNOS is a homodimer with heme as a prosthetic group controlling subunit dimerization and the quaternary structure of nNOS (Klatt et al., 1996). In contrast heme-deficient enzyme (apo-nNOS) is an inactive monomer which degrades rapidly *in vitro* (Dunbar et al., 2004). The amount of nNOS protein in neurons after 72 h inhibition of heme

Molecular Pharmacology Fast Forward. Published on February 15, 2011 as DOI: 10.1124/mol.110.069831
This article has not been copyedited and formatted. The final version may differ from this version.

synthesis was similar in heme-depleted and control cultures (Figure 8B), consistent with nNOS being in a stable and active homodimer in SA-treated cultures at 72 h.

Heme-oxygenase-1 (HO-1) heme serves as both the substrate for the enzyme and the prosthetic group. The amount of HO-1 protein in the microsomal fraction of neuronal lysates was not reduced in the SA-treated neurons (Figure 8C), suggesting that HO-1 basal expression was not affected when total cellular heme was decreased by ~17%.

Cytochromes P450 (CYP450) are drug and steroid-metabolizing enzymes expressed in various tissues including brain. Two isoforms CYP1A1 and CYP4x1(Al-Anizy et al., 2006) were detected in the microsomal fraction by immunoblotting (Figure 8D, E). No differences in protein expression were seen between control and SA-treated for 24 h cultures. Heme also is a positive modulator of CYPs gene transcription and low heme concentration may be a limiting factor for gene expression (Dwarki et al., 1987). We monitored *CYP4x4* gene expression in cultures with inhibited heme synthesis for up to 14 days and did not observe any down-regulation (Figure 8F). Collectively, these data show that heme bound in mitochondrial and others major hemoproteins, such as sGC, nNOS, CYP1a1 and CYP4x1, remained in this state associated with proteins after reduction of heme synthesis by ~50% and depletion of the regulatory heme pool.

Molecular Pharmacology Fast Forward. Published on February 15, 2011 as DOI: 10.1124/mol.110.069831
This article has not been copyedited and formatted. The final version may differ from this version.

Discussion

We previously showed that heme deficiency in primary neurons causes neuronal degeneration (Chernova et al., 2007), however the mechanisms triggering neuronal damage are not well understood. Here we explored the mechanisms by which a deficit of heme affects synaptic function at an early stage of neurodegeneration, prior to neurite fragmentation in primary neurons. We have shown early loss of NMDAR function which correlated with reduced phosphorylation of NR2B subunits. Reduced NMDAR currents and Ca^{2+} influx affected NMDAR-dependent cGMP production and were accompanied by deficient formation of dendritic spines. In this study we used selective and specific inhibition of the second enzyme ALAD in the heme synthetic pathway which remains the optimal means of modulating intracellular heme *in vivo* and *in vitro* (Zhu Y, 2002). ALAS1 is the first and rate limiting enzyme, and consistent with depletion of the regulatory heme pool we monitored increased expression of this gene (Sassa and Nagai, 1996) and protein (Zheng et al., 2008), which is the generally accepted approach to reflect "free" heme levels (Raghuram et al., 2007). In our model the rate of heme synthesis was reduced by ~50% while total intracellular heme was reduced by ~17%, suggesting strong homeostatic mechanisms and supporting previous studies of heme turnover and transport (Maines and Gibbs, 2005). However, the reduction of heme cannot be attributed to reduction of the regulatory pool alone, which has been estimated as <100nM (Sassa and Nagai, 1996). This decrease could be explained by depletion of the regulatory pool and heme from cellular storage. Such heme storage was demonstrated in astrocytes and involved a reputed heme transporter HCP1 (Dang et al., 2010). It is plausible that core functions utilising co-factor heme (e.g. respiratory chain in mitochondrial cytochromes) would be protected by homeostatic mechanisms.

The dynamics of heme depletion in neurons were reflected by apparent reduction of regulatory heme within hours, whereas heme bound in hemoproteins remained at sufficient levels. Mitochondrial

Molecular Pharmacology Fast Forward. Published on February 15, 2011 as DOI: 10.1124/mol.110.069831
This article has not been copyedited and formatted. The final version may differ from this version.

hemoproteins were not affected in the neurons with impaired synthesis and mitochondrial function was not compromised for up to 6 days. This is consistent with the fact that the dissociation constant of mitochondrial hemoprotein heme is $<10^{-13}$ M and "free" heme concentration is estimated at 10^{-7} M (Sassa, 2004). Therefore "free" heme could be lowered by several orders of magnitude before depletion of bound heme occurred. Furthermore, heme is covalently bound in some hemoproteins, and depletion would probably only occur with turnover of the protein. Heme was not depleted from sGC because cGMP production did not change when Ca^{2+}-dependent part of the pathway was by-passed. nNOS protein amounts were unaltered in SA-treated cultures indicating sufficient heme levels to form nNOS homodimers and prevent protein degradation. The amounts of CYP1A1 and CYP4X1 proteins in microsomal fraction remained similar in control and treated cells. Impaired heme levels are believed to decrease CYP450 function via incomplete saturation of apoprotein (Jover et al., 2000), cytosolic persistence of the protein (Meyer et al., 2005) and involvement of heme in transcriptional regulation (Dwarki et al., 1987). Our data did not contradict these suggestions but indicated that more time is required to develop heme deficiency in these functional compartments.

In contrast to hemoproteins, the regulatory pool of heme was depleted promptly after starting treatment and resulted in NMDAR dysfunction. After 24 h of SA treatment NMDA-evoked current was decreased by more than 50%, similar to reduction monitored in the chronic model after 12 days of inhibition. This reduction cannot be related to a direct effect of SA on the receptor because in the presence of heme SA-treated neurons showed a large response to NMDA, similar to control. High permeability of NMDAR for Ca^{2+} places the receptor in the upstream part of various signalling pathways. Physiological levels of synaptic NMDA receptor activation promote survival of many types of neurons and increase their resistance to cellular damage (Hardingham and Bading, 2003). A marked decrease of Ca^{2+} influx in response to NMDA also reflects receptor dysfunction after reduction of heme and is consistent with diminished current. Ca^{2+} can enter cells through many pathways, including neurotransmitter-gated ion channels (NMDAR), Ca^{2+}- permeable subtypes of AMPA receptors, and voltage-dependent Ca^{2+}

Molecular Pharmacology Fast Forward. Published on February 15, 2011 as DOI: 10.1124/mol.110.069831
This article has not been copyedited and formatted. The final version may differ from this version.

channels. There was no reduction in basal Ca^{2+} concentration in treated cells that can be attributed to compensatory Ca^{2+}flow through other receptors, whereas stimulation of NMDAR failed to produce an adequate response. The more sensitive radioimmunoassay of cGMP production detected reduction of NMDAR function even earlier. NMDAR-dependent cGMP production declined as inhibition of heme synthesis continued, suggesting that reduced cGMP concentration itself could contribute to development of neurodegeneration in the chronic model. However, NMDAR functional failure was an earlier change in neurons with depleted regulatory heme and may have triggered alterations of many Ca^{2+}-dependent signalling pathways.

NMDARs play an important role in dendritic spine formation and maintenance. Elongation of existing spines and formation of new filopodia can be blocked by NMDAR antagonists (Shi et al., 2005). Decrease in Ca^{2+} influx affects organisation of cytoskeleton, trafficking of PSD components and recycling of proteins (Nimchinsky et al., 2002), thereby affecting spine formation. Reduction of spines after inhibition of heme synthesis could be another consequence of NMDR dysfunction. NR2B phosphorylation-dependent recovery of spine formation by heme indicates that NMDAR failure causes spine formation deficit, however we cannot exclude interactions of heme with other proteins. Ca^{2+} current through the NMDAR is largely regulated by its NR2B subunit (Krapivinsky et al., 2003) and tyrosine phosphorylation of NR2B is essential to sustain elevation of neuronal Ca^{2+} current (Viviani et al., 2006). We have shown that a marked decrease in NR2B tyrosine phosphorylation was an early change after reduction of regulatory heme in neurons. Similar to NMDA-evoked current, NR2B phosphorylation was rescued by exogenous heme, suggesting a coupling of these recovery mechanisms. Inhibition of SFKs abolished the rescue effect of heme on NMDAR currents providing further evidence of the mechanistic link. Replenishment of heme concentration could reverse early synaptic changes but only if NR2B phosphorylation was resumed. This, and additive effects of PP2 and SA on NR2B phosphorylation, suggest that heme is involved in maintaining NMDAR function via its phosphorylation. Heme modulates NMDAR function in an acute signalling mode, suggesting a direct

Molecular Pharmacology Fast Forward. Published on February 15, 2011 as DOI: 10.1124/mol.110.069831
This article has not been copyedited and formatted. The final version may differ from this version.

interaction, probably within the NMDAR complex and with involvement of SFKs. Exogenous heme alters phosphorylation status of tyrosine kinases in heme-deficient cells (Yao et al., 2010). Src and Jak2 phosphorylations (Tyr530 and Tyr1007 respectively) were increased by heme, and the first has an inhibitory effect on activity of Src and the latter activates JAK2. NR2B phosphorylation at Tyr1252 and Tyr1336 monitored in our study is regulated by Fyn member of SFKs (Nakazawa et al., 2001).There is an evidence of JAK2 crosstalk with SFKs (Jiang et al., 2008), however it requires further clarification of how heme, JAK2 and NMDAR may interact. Interestingly, a mitochondrial protein NADH dehydrogenase subunit 2 (ND2) was recently found to act as an adapter protein anchoring Src to the NMDAR thereby playing a crucial role for Src regulation of synaptic NMDAR activity. ND2 is a subunit of complex I in mitochondria, but in the brain interacts with Src outside this organelle (Gingrich et al., 2004). Using hemin-agarose affinity chromatography of neuronal lysates followed by proteomics analysis we identified a number of putative heme-binding proteins, including partners of NMDAR complex and constituents of mitochondrial complexes I and II which can be potential sites for regulation (supplemental table 1). Heme binding resulting in conformational changes of a target protein (e.g., a kinase or a protein facilitating a phosphorylation) is a plausible mechanism of the rapid increase of NMDAR currents by heme. Further systematic examination is required to identify exact targets of heme interactions with synaptic proteins.

Subunit-specific phosphorylation also controls differentially the trafficking and surface expression of NMDARs (Cull-Candy and Leszkiewicz, 2004), and monitoring these phosphorylations in heme deficient neurons will be addressed in future studies aimed of the relationships in the NMDAR complex in heme-deficiency induced neurodegeneration. The alterations in NMDAR signalling seen in heme depleted neurons could be the trigger for neurite decay. Functional and molecular connections of NMDARs with other receptors, such as AMPA and metabotropic glutamate receptors, are very complex and at this stage we cannot exclude contributions from other receptors and synaptic proteins to neuronal decay in heme deficient cultures. However, rapid and reversible changes in NMDAR function and in

Molecular Pharmacology Fast Forward. Published on February 15, 2011 as DOI: 10.1124/mol.110.069831
This article has not been copyedited and formatted. The final version may differ from this version.

phosphorylation of its regulatory subunit correlated with availability of heme, couple the receptor and heme in a signalling mode.

Together these findings lead to the conclusion that depletion of regulatory heme rapidly compromises NR2B phosphorylation and causes dysfunction of NMDARs; this compromises calcium-dependent signalling pathways, triggers changes in cGMP production and dendritic spine formation. Synaptic changes precede depletion of heme from major hemoproteins. Further exploration of heme interaction with NMDAR complex and understanding how exactly the effects of heme are exerted and could be modulated by drugs, may provide new insights into reversal of neurodegeneration.

Molecular Pharmacology Fast Forward. Published on February 15, 2011 as DOI: 10.1124/mol.110.069831
This article has not been copyedited and formatted. The final version may differ from this version.

Acknowledgments

We thank the members of the University of Leicester Biomedical Services staff for their assistance; Dr. Michael J. Schell (Dept. of Pharmacology, Uniformed Services University, Bethesda) for the gift of FLAG-tagged tdTomato construct and Dr. D Bell (School of Biology, University of Nottingham) for the gift of CYP4x1 antibody .

Authorship Contributions.

Participated in research design: Tatyana Chernova, Andrew G. Smith and Ian D. Forsythe

Conducted experiments: Chernova T, Steinert R.J., Richards P., Mistry R,

Contributed new reagents or analytic tools: Jukes-Jones R, Cain K

Wrote or contributed to the writing of the manuscript: Chernova T, Steinert R.J., Smith A.G. and Forsythe I.D.

Molecular Pharmacology Fast Forward. Published on February 15, 2011 as DOI: 10.1124/mol.110.069831
This article has not been copyedited and formatted. The final version may differ from this version.

References

Al-Anizy M, Horley NJ, Kuo CW, Gillett LC, Laughton CA, Kendall D, Barrett DA, Parker T and Bell DR (2006) Cytochrome P450 Cyp4x1 is a major P450 protein in mouse brain. *FEBS J* **273**(5):936-947.

Atamna H and Frey WH, 2nd (2004) A role for heme in Alzheimer's disease: heme binds amyloid beta and has altered metabolism. *Proc Natl Acad Sci U S A* **101**(30):11153-11158.

Ballou DP, Zhao Y, Brandish PE and Marletta MA (2002) Revisiting the kinetics of nitric oxide (NO) binding to soluble guanylate cyclase: the simple NO-binding model is incorrect. *Proc Natl Acad Sci U S A* **99**(19):12097-12101.

Boekhoorn K, Terwel D, Biemans B, Borghgraef P, Wiegert O, Ramakers GJ, de Vos K, Krugers H, Tomiyama T, Mori H, Joels M, van Leuven F and Lucassen PJ (2006) Improved long-term potentiation and memory in young tau-P301L transgenic mice before onset of hyperphosphorylation and tauopathy. *J Neurosci* **26**(13):3514-3523.

Chernova T, Nicotera P and Smith AG (2006) Heme deficiency is associated with senescence and causes suppression of N-methyl-D-aspartate receptor subunits expression in primary cortical neurons. *Mol Pharmacol* **69**(3):697-705.

Chernova T, Steinert JR, Guerin CJ, Nicotera P, Forsythe ID and Smith AG (2007) Neurite degeneration induced by heme deficiency mediated via inhibition of NMDA receptor-dependent extracellular signal-regulated kinase 1/2 activation. *J Neurosci* **27**(32):8475-8485.

Cull-Candy SG and Leszkiewicz DN (2004) Role of distinct NMDA receptor subtypes at central synapses. *Sci STKE* **2004**(255):re16.

Dang TN, Bishop GM, Dringen R and Robinson SR (2010) The putative heme transporter HCP1 is expressed in cultured astrocytes and contributes to the uptake of hemin. *Glia* **58**(1):55-65.

Dunbar AY, Kamada Y, Jenkins GJ, Lowe ER, Billecke SS and Osawa Y (2004) Ubiquitination and degradation of neuronal nitric-oxide synthase in vitro: dimer stabilization protects the enzyme from proteolysis. *Mol Pharmacol* **66**(4):964-969.

Dwarki VJ, Francis VN, Bhat GJ and Padmanaban G (1987) Regulation of cytochrome P-450 messenger RNA and apoprotein levels by heme. *J Biol Chem* **262**(35):16958-16962.

Ethell IM and Pasquale EB (2005) Molecular mechanisms of dendritic spine development and remodeling. *Prog Neurobiol* **75**(3):161-205.

Gingrich JR, Pelkey KA, Fam SR, Huang Y, Petralia RS, Wenthold RJ and Salter MW (2004) Unique domain anchoring of Src to synaptic NMDA receptors via the mitochondrial protein NADH dehydrogenase subunit 2. *Proc Natl Acad Sci U S A* **101**(16):6237-6242.

Hardingham GE and Bading H (2003) The Yin and Yang of NMDA receptor signalling. *Trends Neurosci* **26**(2):81-89.

Ishii DN and Maniatis GM (1978) Haemin promotes rapid neurite outgrowth in cultured mouse neuroblastoma cells. *Nature* **274**(5669):372-374.

Jiang L, Li Z and Rui L (2008) Leptin stimulates both JAK2-dependent and JAK2-independent signaling pathways. *J Biol Chem* **283**(42):28066-28073.

Jover R, Hoffmann F, Scheffler-Koch V and Lindberg RL (2000) Limited heme synthesis in porphobilinogen deaminase-deficient mice impairs transcriptional activation of specific cytochrome P450 genes by phenobarbital. *Eur J Biochem* **267**(24):7128-7137.

Kannan M, Steinert JR, Forsythe ID, Smith AG and Chernova T (2010) Mevastatin accelerates loss of synaptic proteins and neurite degeneration in aging cortical neurons in a heme-independent manner. *Neurobiol Aging* **31**(9):1543-1553.

Kapoor N, Pant AB, Dhawan A, Dwievedi UN, Gupta YK, Seth PK and Parmar D (2006) Differences in sensitivity of cultured rat brain neuronal and glial cytochrome P450 2E1 to ethanol. *Life Sci* **79**(16):1514-1522.

Klatt P, Pfeiffer S, List BM, Lehner D, Glatter O, Bachinger HP, Werner ER, Schmidt K and Mayer B (1996) Characterization of heme-deficient neuronal nitric-oxide synthase reveals a role for heme in subunit

dimerization and binding of the amino acid substrate and tetrahydrobiopterin. *J Biol Chem* **271**(13):7336-7342.

Krapivinsky G, Krapivinsky L, Manasian Y, Ivanov A, Tyzio R, Pellegrino C, Ben-Ari Y, Clapham DE and Medina I (2003) The NMDA receptor is coupled to the ERK pathway by a direct interaction between NR2B and RasGRF1. *Neuron* **40**(4):775-784.

Maines MD and Gibbs PE (2005) 30 some years of heme oxygenase: from a "molecular wrecking ball" to a "mesmerizing" trigger of cellular events. *Biochem Biophys Res Commun* **338**(1):568-577.

Mallucci GR (2009) Prion neurodegeneration: starts and stops at the synapse. *Prion* **3**(4):195-201.

Meyer RP, Lindberg RL, Hoffmann F and Meyer UA (2005) Cytosolic persistence of mouse brain CYP1A1 in chronic heme deficiency. *Biol Chem* **386**(11):1157-1164.

Moon IS, Apperson ML and Kennedy MB (1994) The major tyrosine-phosphorylated protein in the postsynaptic density fraction is N-methyl-D-aspartate receptor subunit 2B. *Proc Natl Acad Sci U S A* **91**(9):3954-3958.

Nakazawa T, Komai S, Tezuka T, Hisatsune C, Umemori H, Semba K, Mishina M, Manabe T and Yamamoto T (2001) Characterization of Fyn-mediated tyrosine phosphorylation sites on GluR epsilon 2 (NR2B) subunit of the N-methyl-D-aspartate receptor. *J Biol Chem* **276**(1):693-699.

Nimchinsky EA, Sabatini BL and Svoboda K (2002) Structure and function of dendritic spines. *Annu Rev Physiol* **64**:313-353.

Ogawa K, Sun J, Taketani S, Nakajima O, Nishitani C, Sassa S, Hayashi N, Yamamoto M, Shibahara S, Fujita H and Igarashi K (2001) Heme mediates derepression of Maf recognition element through direct binding to transcription repressor Bach1. *Embo J* **20**(11):2835-2843.

Raghuram S, Stayrook KR, Huang P, Rogers PM, Nosie AK, McClure DB, Burris LL, Khorasanizadeh S, Burris TP and Rastinejad F (2007) Identification of heme as the ligand for the orphan nuclear receptors REV-ERBalpha and REV-ERBbeta. *Nat Struct Mol Biol* **14**(12):1207-1213.

Sassa S (2004) Why heme needs to be degraded to iron, biliverdin IXalpha, and carbon monoxide? *Antioxid Redox Signal* **6**(5):819-824.

Sassa S and Nagai T (1996) The role of heme in gene expression. *Int J Hematol* **63**(3):167-178.

Shi GX, Han J and Andres DA (2005) Rin GTPase couples nerve growth factor signaling to p38 and b-Raf/ERK pathways to promote neuronal differentiation. *J Biol Chem* **280**(45):37599-37609.

Shinjyo N and Kita K (2006) Up-regulation of heme biosynthesis during differentiation of Neuro2a cells. *J Biochem* **139**(3):373-381.

Soto C and Estrada LD (2008) Protein misfolding and neurodegeneration. *Arch Neurol* **65**(2):184-189.

Tang XD, Xu R, Reynolds MF, Garcia ML, Heinemann SH and Hoshi T (2003) Haem can bind to and inhibit mammalian calcium-dependent Slo1 BK channels. *Nature* **425**(6957):531-535.

Viviani B, Gardoni F, Bartesaghi S, Corsini E, Facchi A, Galli CL, Di Luca M and Marinovich M (2006) Interleukin-1beta released by gp120 drives neural death through tyrosine phosphorylation and trafficking of NMDA receptors. *J Biol Chem* **281**(40):30212-30222.

White KA and Marletta MA (1992) Nitric oxide synthase is a cytochrome P-450 type hemoprotein. *Biochemistry* **31**(29):6627-6631.

Wishart TM, Parson SH and Gillingwater TH (2006) Synaptic vulnerability in neurodegenerative disease. *J Neuropathol Exp Neurol* **65**(8):733-739.

Yao X, Balamurugan P, Arvey A, Leslie C and Zhang L (2010) Heme controls the regulation of protein tyrosine kinases Jak2 and Src. *Biochem Biophys Res Commun* **403**(1):30-35.

Zheng J, Shan Y, Lambrecht RW, Donohue SE and Bonkovsky HL (2008) Differential regulation of human ALAS1 mRNA and protein levels by heme and cobalt protoporphyrin. *Mol Cell Biochem* **319**(1-2):153-161.

Zhu Y HT, Ye W, Zhang L. (2002) Heme deficiency interferes with the Ras-mitogen-activated protein kinase signaling pathway and expression of a subset of neuronal genes. *Cell Growth Differ* **13**(9):431-439.

Molecular Pharmacology Fast Forward. Published on February 15, 2011 as DOI: 10.1124/mol.110.069831
This article has not been copyedited and formatted. The final version may differ from this version.

Legends for figures

Figure 1. Reduction of neuronal intracellular heme follows treatment with an inhibitor of heme synthesis, succinyl acetone (SA). Neurons maintained for 12DIV were treated with 250μM SA for 9-24 h with or without exogenous heme. (A) Rate of heme synthesis. Treated and control neurons were incubated with ^{3}H-ALA for 24 h on day 14 and then labelled heme was extracted and measured (n = 5), ** $p< 0.01$. (B) Concentration of intracellular heme in control, treated with SA and co-treated with SA and 0.1μM heme (n = 5), * statistically different, $p<0.05$. (C) Up-regulation of *ALAS1* as a result of reduction of "free" heme in the cells occurs within hours after inhibition of heme synthesis. *ALAS1* expression measured by Real Time PCR in control, SA-treated and co-treated with SA and 0.1μM heme. Data denote mean ± SD of at least three independent experiments. * Indicates statistically different from control group, $p<0.05$, # statistically different from 9h time-point. (D) Increase of ALAS1 protein in response to inhibition of heme synthesis for 16 and 24 hours. Expression of ALAS1 in microsomal fraction in control and treated with SA neurons detected by western blot, lower panel shows quantification of immunoblotting with ALAS1 expression normalized against α-tubulin, data denote mean ± SD of at least three independent experiments.

Figure 2. Reduction of intracellular heme decreases NR2B tyrosine phosphorylation; exogenous heme reverses this change and the rescue effect requires SFKs activity. Neurons were treated with 250μM SA for 24 h with or without exogenous heme and with or without Src kinase inhibitor PP2 at 13DIV. (A) Phosphorylation levels of NR2B at Y1252 and Y1336 corresponding to the above conditions were examined by Western blot, images show representative blots. The same blots were re-probed for α-tubulin. (B) Quantification of band intensities obtained using densitometry and Image Quant 5.2 software and normalized to α-tubulin. Each column is the mean normalized expression of protein ± SD of at least three independent experiments. * Indicates statistically different from control group, $p< 0.05$,

Molecular Pharmacology Fast Forward. Published on February 15, 2011 as DOI: 10.1124/mol.110.069831
This article has not been copyedited and formatted. The final version may differ from this version.

statistically different, $p< 0.05$. (C-N) Confocal micrographs of maximum projection *Z* series of cultured neurons at 13DIV stained for phospho-NR2B (Y1252 and Y1336, top and bottom panels respectively, red) and for postsynaptic density-95 (PSD-95, green), the nuclei were stained with DAPI (blue). (C, I) control cultures; (D) and (J), cultures treated with 50nM PP2 for 2 h; (E) and (K), SA treated for 18 h; (F) and (L) were treated with SA and PP2 for 18 h; (G), (H), (M) and (N) were treated with SA and heme for 18h in presence (H, N) or absence (G, M) of PP2.

Figure 3. Inhibition of heme synthesis promptly leads to suppression of NMDA-evoked currents; heme re-admission reverses this change. (A) Whole-cell currents evoked by pressure application of NMDA (indicated by arrow; 100μM, 20PSI, 30ms) to cortical neurons at holding potentials of -60 and +40 mV in control (top), and from neurons treated with SA for 24h (upper middle), SA in the presence of heme (low middle) and control neurons treated with heme (bottom). (B) I-V relationships for recorded NMDA currents under the same conditions. SA treatment reduced NMDA-evoked current over all voltages tested (SA) but not in the cells co-treated with heme. (C) Summary graph of NMDA currents at +40mV holding potential under the three conditions. Data denote mean ± SEM of at least five different cells (n shown in each bar). Significance assessed using ANOVA, * Indicates $p< 0.01$.

Figure 4. Heme depletion reduces NMDA-evoked Ca^{2+} influx and Ca^{2+}-dependent cGMP production. The ratio of fluorescence at 340 and 380 nm excitation in the cell soma was used as a measure of $[Ca^{2+}]_i$. (A) Representative 340/380nm ratio traces of NMDA-evoked intracellular Ca^{2+} ($[Ca^{2+}]_i$) in control cells (Ctrl), cells treated with SA for 24 and 44 h at 12-13DIV. (B) NMDA-evoked Ca^{2+} responses (Δratio, peak - basal) are reduced after 24 h of SA treatment but rescued by exogenous heme. Data denote mean ± SEM of at least three cells from each of the three independent experiments (n shown in each bar). (C) Ca^{2+}- dependent production of cGMP is decreased in neurons with reduced intracellular heme. Neurons (12-13DIV) were treated with 250μM SA and harvested after 16, 24, 30 or 42 h of treatment, cGMP production was monitored by radioimmunoassay, measurements are expressed

Molecular Pharmacology Fast Forward. Published on February 15, 2011 as DOI: 10.1124/mol.110.069831
This article has not been copyedited and formatted. The final version may differ from this version.

as % of cGMP production in control cultures. Data denote mean ± SD of three independent experiments. * Statistically different from control group, $p< 0.05$; # statistically different from SA treatment for 16 h, $p <0.05$.

Figure 5. Spine formation is reduced in neurons with deficient intracellular heme and rescued by exogenous heme; the rescue effect is NR2B phosphorylation-dependent. (A-F) Confocal micrographs of maximum projection *Z* series of control (A), treated with SA (B) or SA and heme (C), SA and PP2 (D) and SA, heme and PP2 (E) neurons transfected with FLAG-tagged tdTomato expressing red fluorescent cell-filling to visualize dendritic morphology. (F) Quantification of spines (number per length, n= 16-25), in cultures from three independent experiments *$p<0.05$.

Figure 6. Acute effects of heme on function and phosphorylation of NMDAR. (A) Heme-deficient SA-treated (24h) neurons (n=9) showed a 70% reduction in NMDA-evoked currents (blue diamonds) over a recording time of 13min. When heme (0.1μM) was applied in the bath at 2min (indicated by the arrow) the initial current decline stopped and NMDA-evoked currents were potentiated by 40% over 13min (squares, n=4). Top raw traces indicate representative currents at indicated time points (i-iii). When heme was present in the patch pipette, currents started to increase immediately after patching (triangles, n=3). (B, C) Exogenous heme rapidly restores phosphorylation of NR2B subunit at Y1252 and Y1336 in SA-treated neurons, inhibition of Src kinase abolishes rescue effect of heme. Neurons at 13DIV were treated with 250μM SA for 24h followed by 15min incubation with exogenous heme with or without 2h pre-treatment with Src kinase inhibitor PP2. Phosphorylation levels of NR2B at Y1336 (B) and Y1252 (C) are corresponding to the above conditions were examined by western blot, images show representative blots. The same blots were re-probed for α-tubulin. Lower panels, quantification of band intensities obtained using densitometry and Image Quant 5.2 software and normalized to α-tubulin. Each column is the mean normalized expression of protein ± SD of three independent experiments.

Molecular Pharmacology Fast Forward. Published on February 15, 2011 as DOI: 10.1124/mol.110.069831
This article has not been copyedited and formatted. The final version may differ from this version.

* Indicates statistically different from control group, $p < 0.05$.

Figure 7. Mitochondrial membrane potential was unaffected in neurons with moderately reduced intracellular heme. Control (A) and treated with 250μM SA for 72 h (B) neurons were stained with 5,5',6,6'-tetrachloro-1,1',3,3'-tetraethylbenzimidazoyl carbocyanine iodide (DePsipher™ Kit) and displayed aggregation of the DePsipher within the mitochondria with high $\Delta\Psi m$ (red). (C) ATP production in control and treated cultures with 250μM SA up to 6 days measured by CellTiter-Glo Luminescent Cell Viability Assay. All measurements were conducted in triplicate, ATP concentrations were normalized to total protein content in the samples. Error bars indicate the standard deviation of three samples with the same treatment from at least three independent experiments.

Figure 8. Hemoprotein heme is preserved in neurons following reduction of heme synthesis. (A) cGMP production in the presence of NO donor is maintained in heme-deficient neurons. Concentrations of cGMP in the control and SA-treated cultures were monitored in radioimmunoassay and expressed as fold stimulation in response to NO donor SNAP (the ratio of basal and NO-stimulated cGMP production). Data denote mean ± SD of at least three independent experiments. (B) Expression of nNOS in control and treated neurons, whole cell lysates were separated by native polyacrylamide gel electrophoresis and analysed by immunoblotting. Lower panel shows quantification of nNOS band intensities normalized to α-tubulin, each column is the mean of normalized protein expression ± SD of three independent experiments. (C) Expression of HO-1 in microsomal fraction in control and treated with SA neurons detected by western blot, lower panel shows quantification of immunoblotting with HO-1 expression normalized against microsomal protein P450 reductase; α-tubulin was detected in whole cell lysate before isolation of microsomal fraction, data denote mean ± SD of at least three independent experiments. (D, E) Expression of CYP4x1 and CYP1A1 in microsomal fraction of neurons treated with SA for 24 h compared to control. Lower panels are quantification of western blots,

Molecular Pharmacology Fast Forward. Published on February 15, 2011 as DOI: 10.1124/mol.110.069831
This article has not been copyedited and formatted. The final version may differ from this version.

expression levels are normalized to microsomal protein P450 reductase. Each column is the mean of normalized protein expression ± SD of three independent experiments. (F) Expression of CYP4x1 gene in control, heme-deficient neurons chronically treated with SA (2DIV-14DIV) and neurons treated with SA and heme for 12 days (2DIV-14DIV) measured by real time PCR; β–actin was used as an endogenous reference gene.

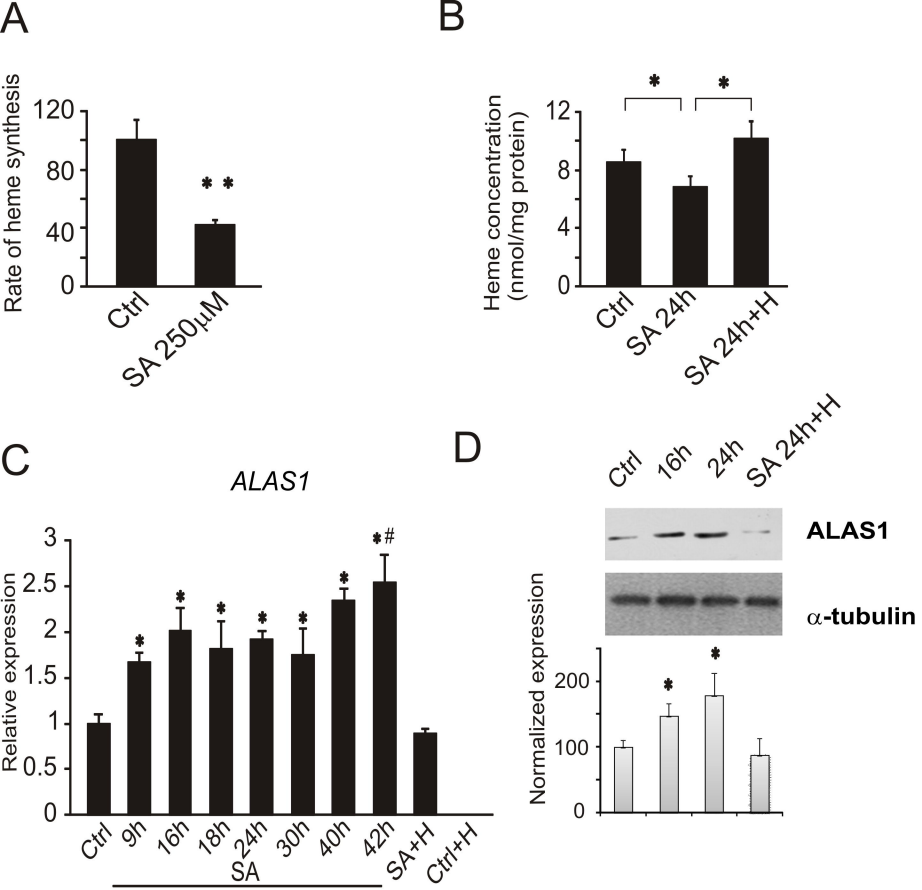
A
Rate of heme synthesis
120
80
40
0
Ctrl
SA 250μM
B
Heme concentration (nmol/mg protein)
12
8
4
0
Ctrl
SA 24h
SA 24h+H
C
ALAS1
Relative expression
3
2.5
2
1.5
1
0.5
0
Ctrl
9h
16h
18h
24h
30h
40h
42h
SA
SA+H
Ctrl+H
D
Ctrl
16h
24h
SA 24h+H
ALAS1
α-tubulin
Normalized expression
200
100
0

Fig. 1

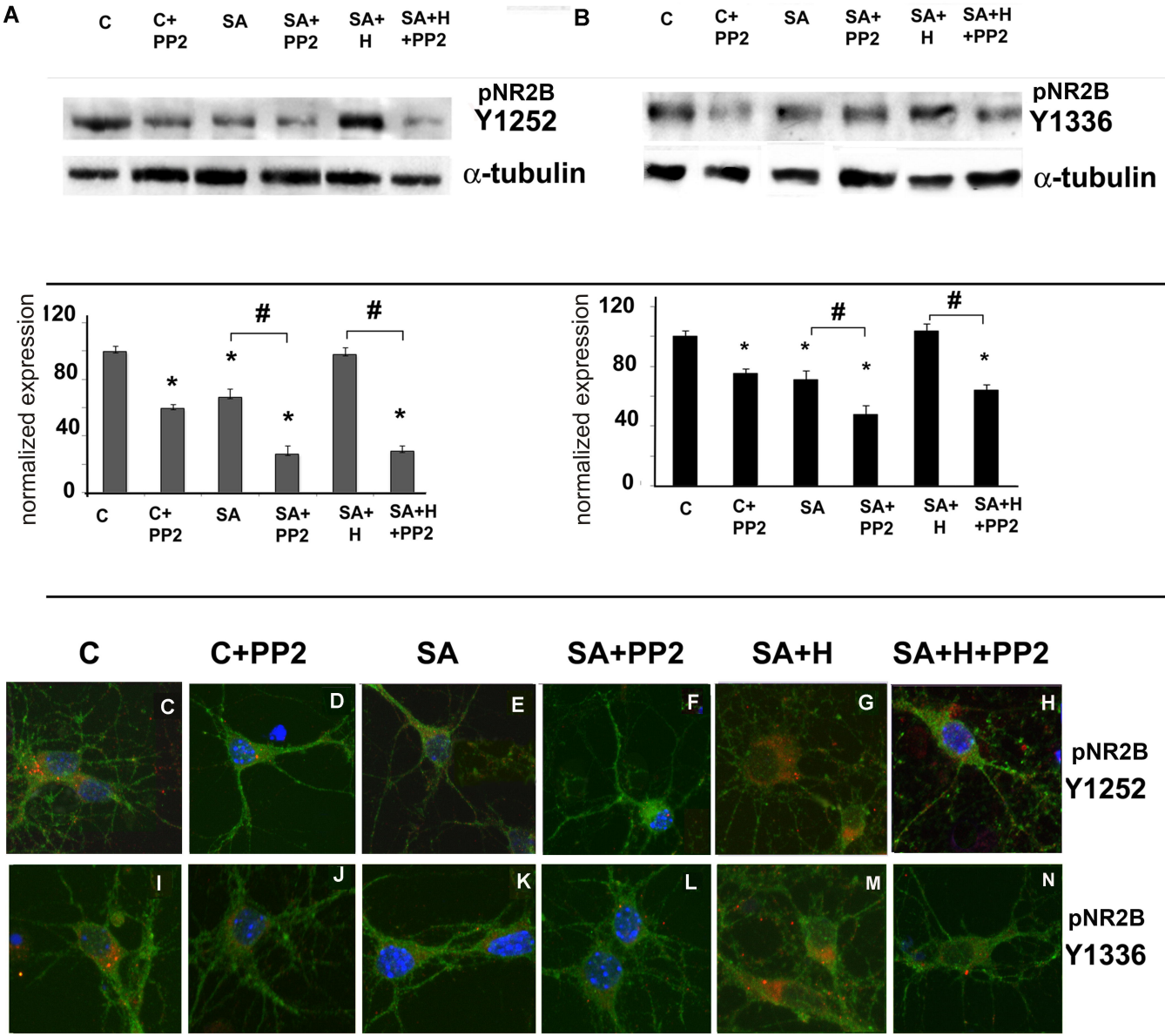
A
C
C+ PP2
SA
SA+ PP2
SA+ H
SA+H +PP2
pNR2B Y1252
α-tubulin
B
C
C+ PP2
SA
SA+ PP2
SA+ H
SA+H +PP2
pNR2B Y1336
α-tubulin
normalized expression
120
80
40
0
#
#
*
C
C+ PP2
SA
SA+ PP2
SA+ H
SA+H +PP2
normalized expression
120
80
40
0
#
#
*
C
C+ PP2
SA
SA+ PP2
SA+ H
SA+H +PP2
C
C+PP2
SA
SA+PP2
SA+H
SA+H+PP2
C
D
E
F
G
H
pNR2B Y1252
I
J
K
L
M
N
pNR2B Y1336

figure 2

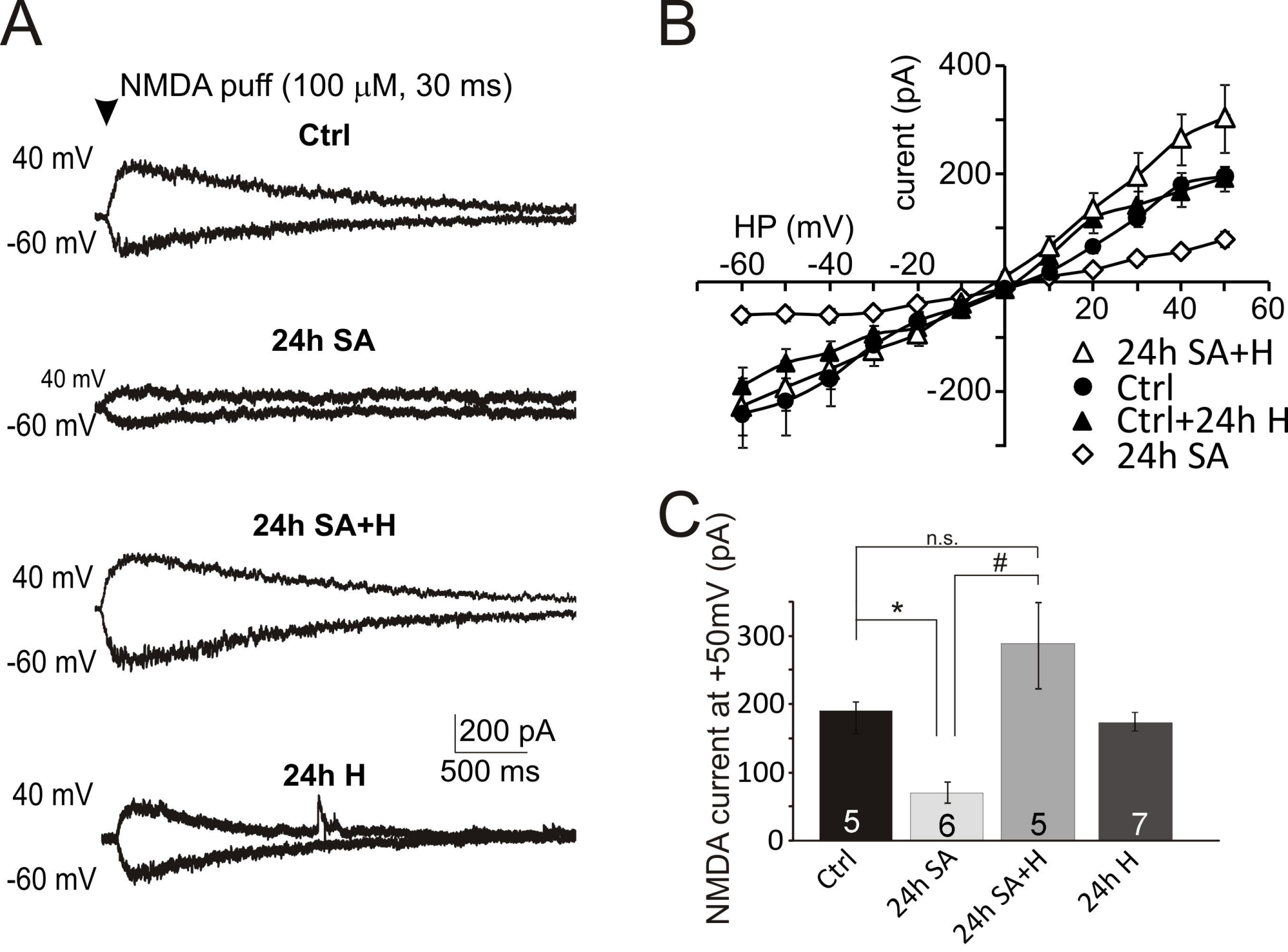
A
NMDA puff (100 μM, 30 ms)
Ctrl
40 mV
-60 mV
24h SA
40 mV
-60 mV
24h SA+H
40 mV
-60 mV
200 pA
500 ms
24h H
40 mV
-60 mV
B
curent (pA)
400
200
-200
HP (mV)
-60
-40
-20
20
40
60
24h SA+H
Ctrl
Ctrl+24h H
24h SA
C
NMDA current at +50mV (pA)
n.s.
#
*
300
200
100
0
5
6
5
7
Ctrl
24h SA
24h SA+H
24h H

figure 3

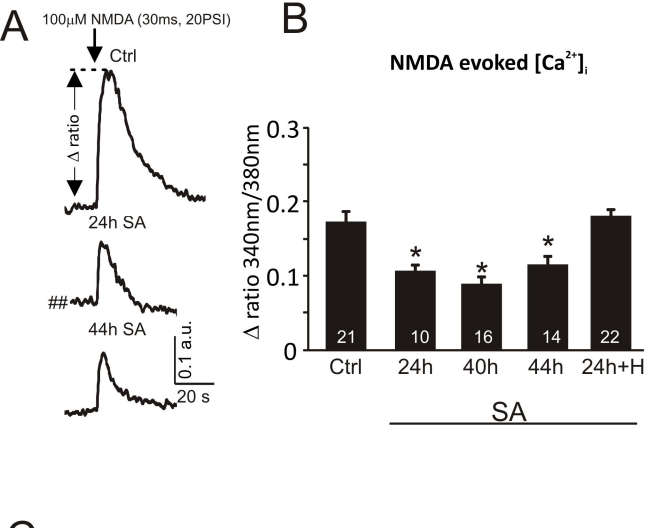
A
100μM NMDA (30ms, 20PSI)
Ctrl
Δ ratio
24h SA
##
44h SA
0.1 a.u.
20 s
B
NMDA evoked [Ca2+]i
Δ ratio 340nm/380nm
0.3
0.2
0.1
0
21
10
16
14
22
Ctrl
24h
40h
44h
24h+H
SA

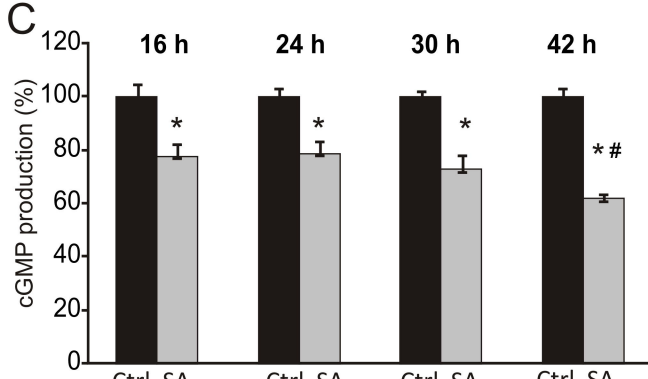
C
16 h
24 h
30 h
42 h
cGMP production (%)
120
100
80
60
40
20
0
Ctrl SA
Ctrl SA
Ctrl SA
Ctrl SA
*
*
*
*#

figure 4

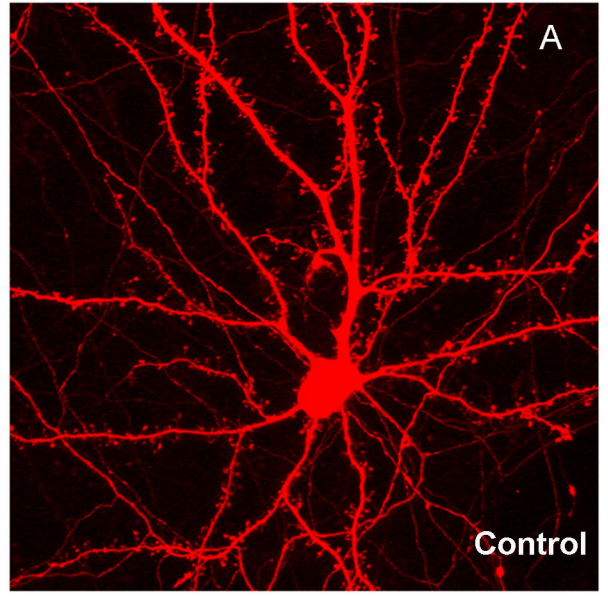
A
Control

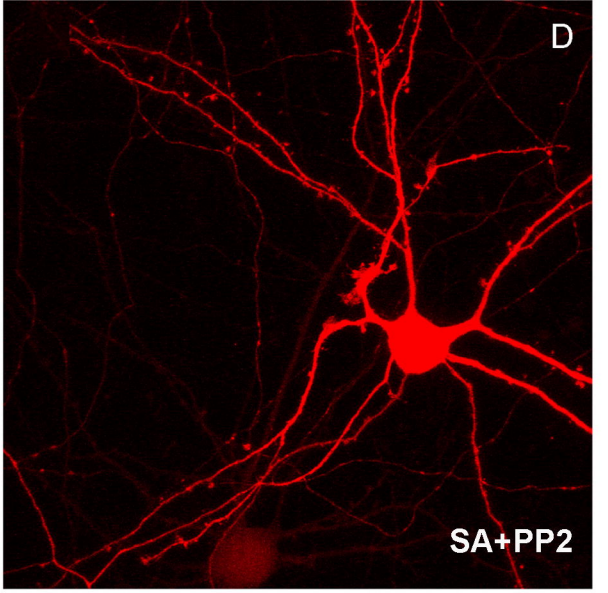
D
SA+PP2

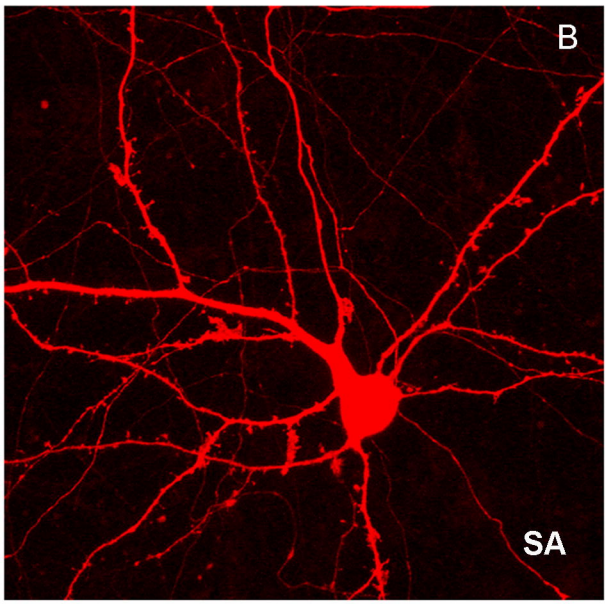
B
SA

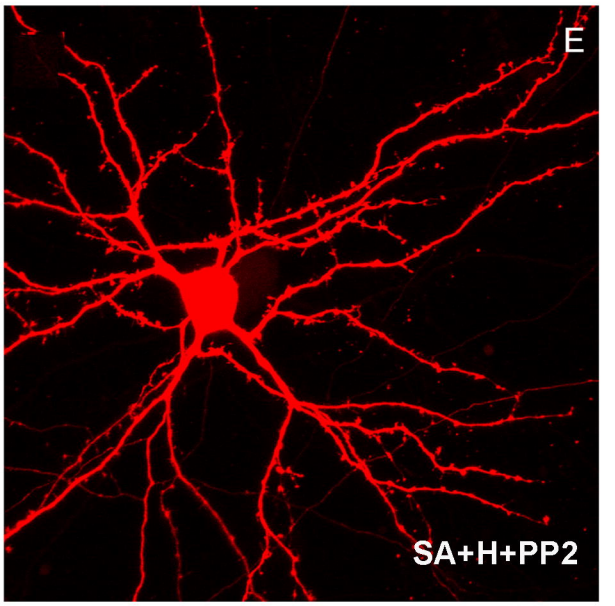
E
SA+H+PP2

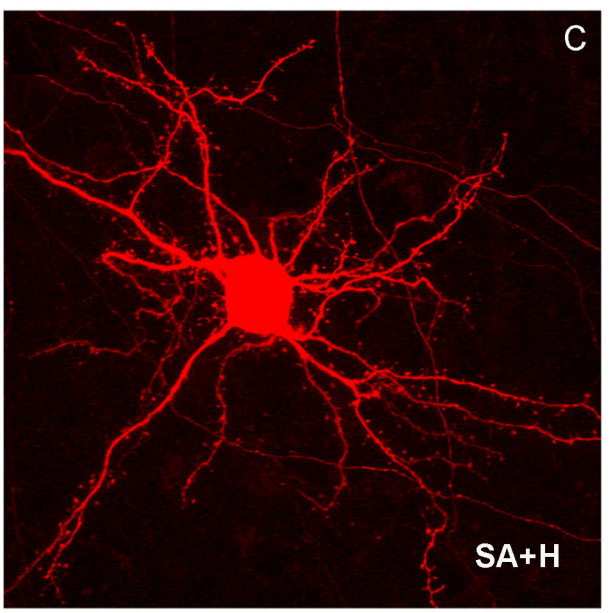
C
SA+H

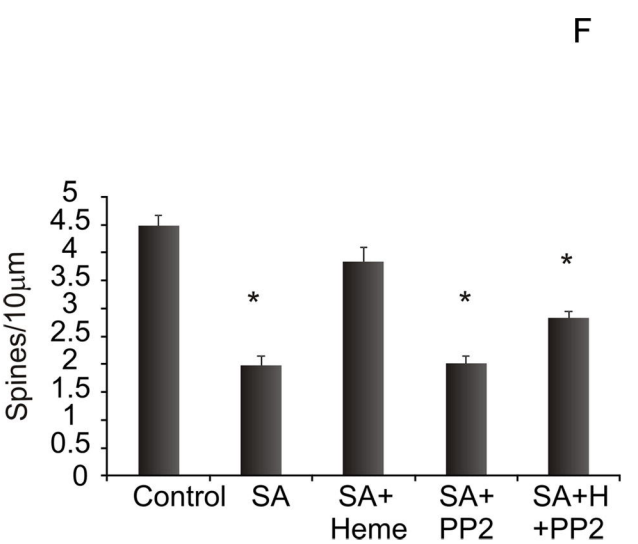
F
Spines/10μm
5
4.5
4
3.5
3
2.5
2
1.5
1
0.5
0
*
*
*
Control
SA
SA+ Heme
SA+ PP2
SA+H +PP2

figure 5

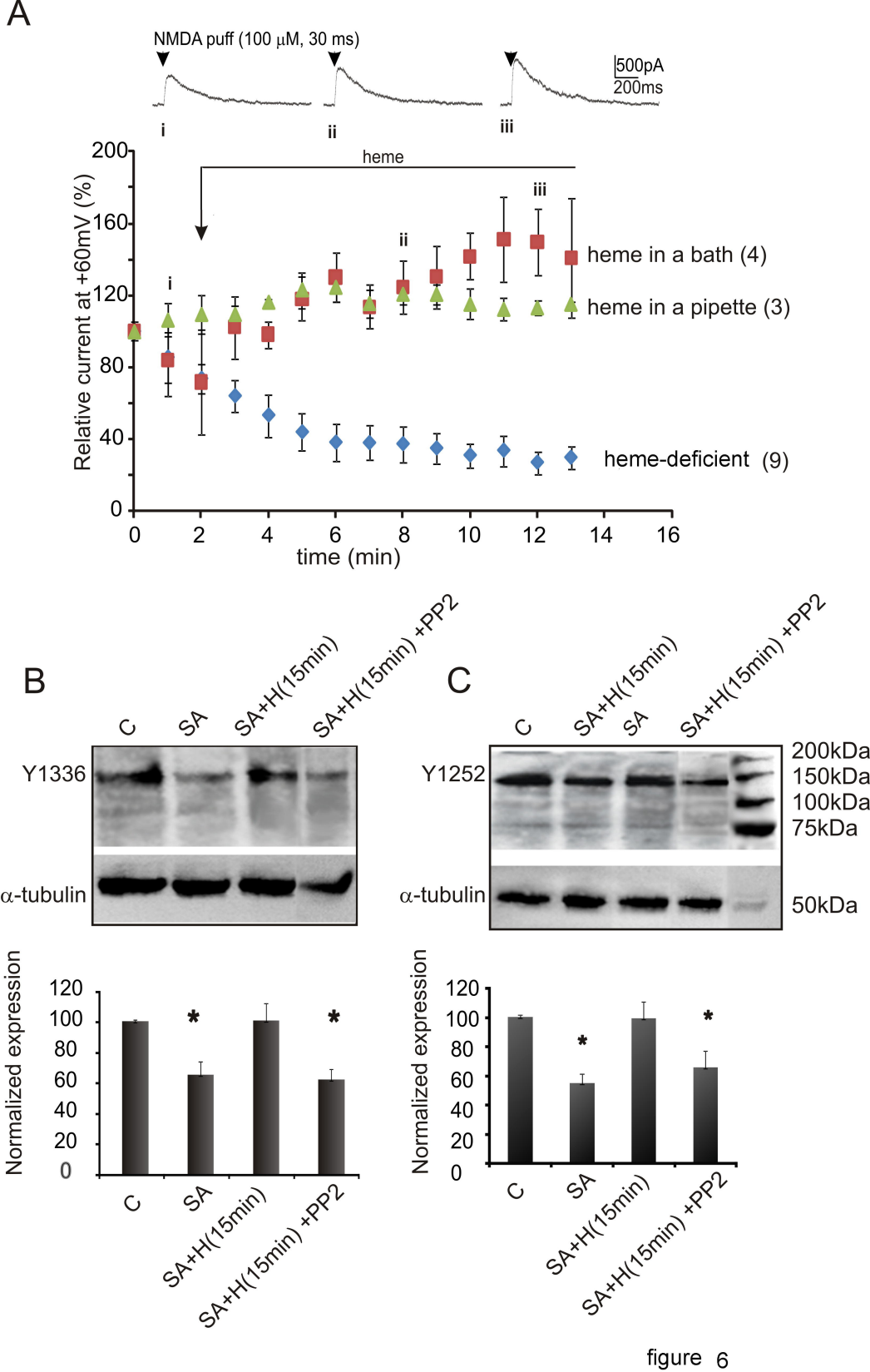
A
NMDA puff (100 μM, 30 ms)
500pA
200ms
i
ii
iii
heme
Relative current at +60mV (%)
time (min)
heme in a bath (4)
heme in a pipette (3)
heme-deficient (9)
B
C
SA+H(15min) +PP2
Y1336
α-tubulin
Y1252
200kDa
150kDa
100kDa
75kDa
50kDa
Normalized expression

figure 6

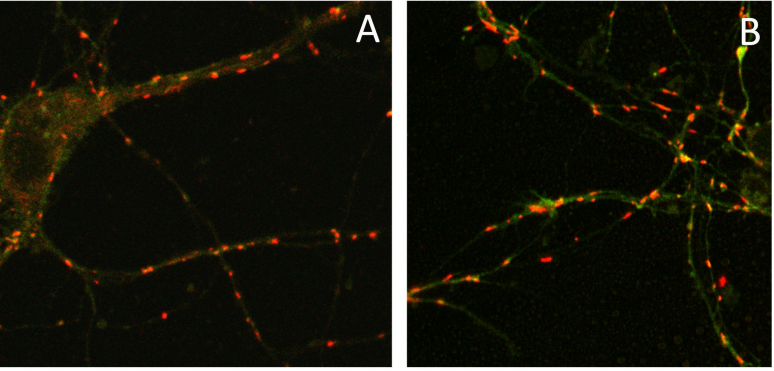
A
B

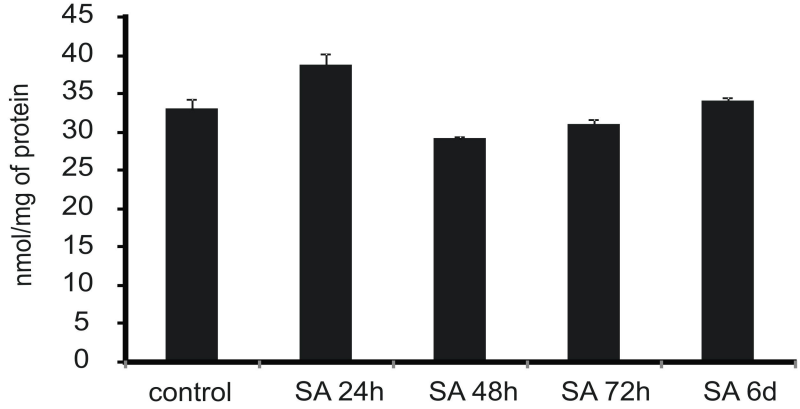
45
40
35
30
25
20
15
10
5
0
nmol/mg of protein
control
SA 24h
SA 48h
SA 72h
SA 6d

figure 7

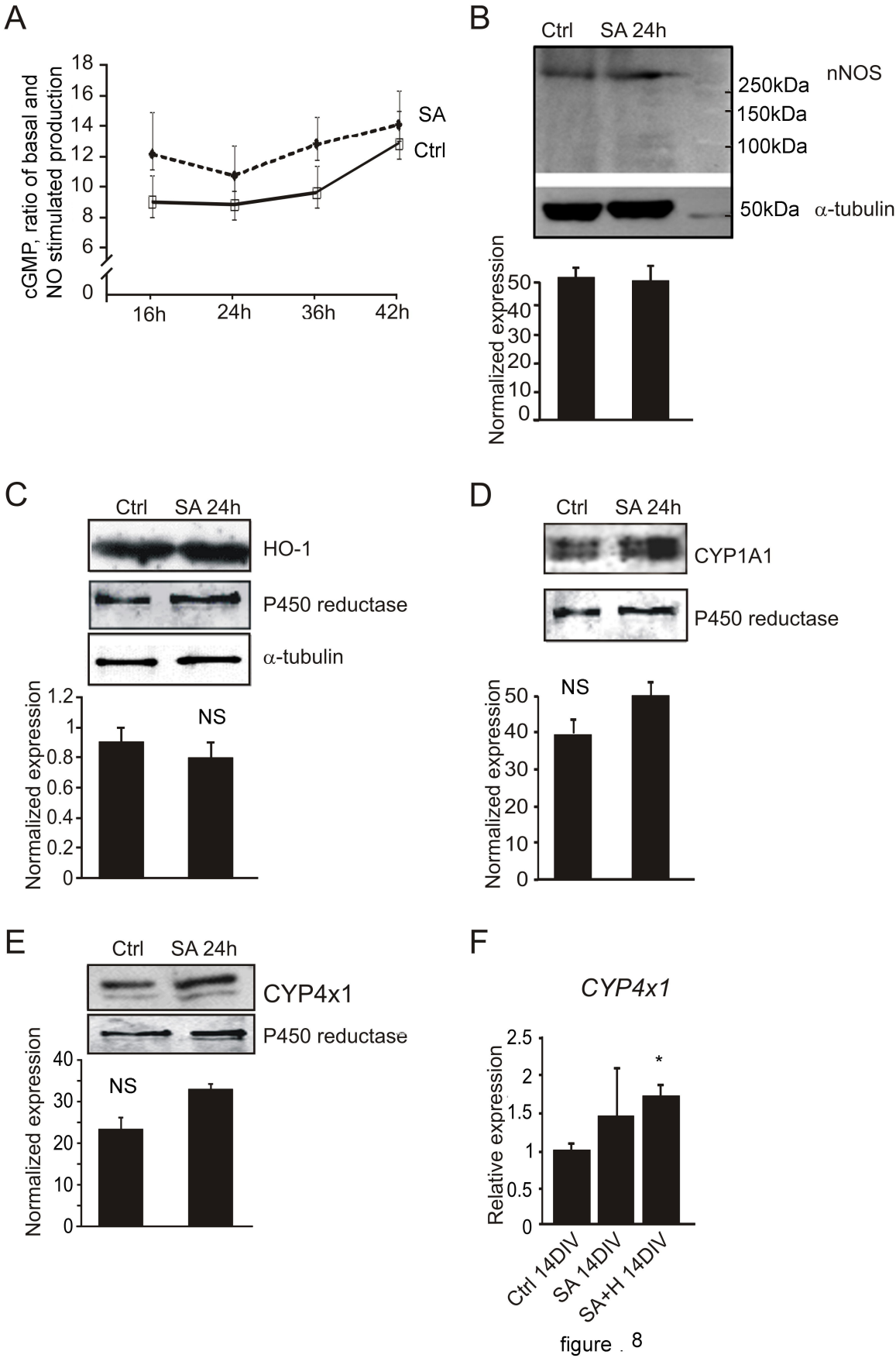
A
cGMP, ratio of basal and NO stimulated production
18
16
14
12
10
8
6
0
16h
24h
36h
42h
SA
Ctrl
B
Ctrl
SA 24h
250kDa
150kDa
100kDa
50kDa
nNOS
α-tubulin
Normalized expression
50
40
30
20
10
0
C
Ctrl
SA 24h
HO-1
P450 reductase
α-tubulin
Normalized expression
1.2
1
0.8
0.6
0.4
0.2
0
NS
D
Ctrl
SA 24h
CYP1A1
P450 reductase
Normalized expression
50
40
30
20
10
0
NS
E
Ctrl
SA 24h
CYP4x1
P450 reductase
Normalized expression
40
30
20
10
0
NS
F
CYP4x1
Relative expression
2.5
2
1.5
1
0.5
0
*
Ctrl 14DIV
SA 14DIV
SA+H 14DIV

figure . 8